AD A067516

LEVEL II

(12)

NW

(14) DRDMI-

TECHNICAL REPORT T-79-1

(6) GYROCOMPASSING ERROR ANALYSIS FOR PERSHING II INERTIAL MEASUREMENT UNIT.

(9) Technical rept.

(10) H. V. White and J. C. Hung
Guidance and Control Directorate
Technology Laboratory

(11) November 1978

(12) 42p.

Approved for public release; distribution unlimited.

U.S. ARMY MISSILE RESEARCH AND DEVELOPMENT COMMAND

Redstone Arsenal, Alabama 35809

DMI FORM 1000, 1 APR 77

393427

79 04 16 022

DISCLAIMER NOTICE

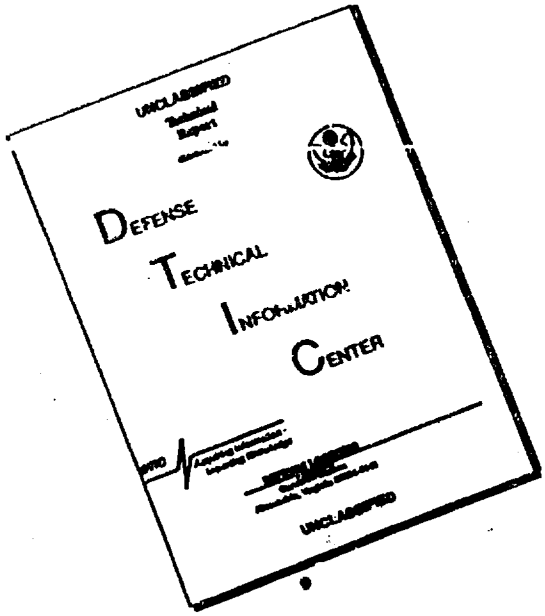

THIS DOCUMENT IS BEST QUALITY AVAILABLE. THE COPY FURNISHED TO DTIC CONTAINED A SIGNIFICANT NUMBER OF PAGES WHICH DO NOT REPRODUCE LEGIBLY.

DISPOSITION INSTRUCTIONS

DESTROY THIS REPORT WHEN IT IS NO LONGER NEEDED. DO NOT RETURN IT TO THE ORIGINATOR.

DISCLAIMER

THE FINDINGS IN THIS REPORT ARE NOT TO BE CONSTRUED AS AN OFFICIAL DEPARTMENT OF THE ARMY POSITION UNLESS SO DESIGNATED BY OTHER AUTHORIZED DOCUMENTS.

TRADE NAMES

USE OF TRADE NAMES OR MANUFACTURERS IN THIS REPORT DOES NOT CONSTITUTE AN OFFICIAL INDORSEMENT OR APPROVAL OF THE USE OF SUCH COMMERCIAL HARDWARE OR SOFTWARE.

UNCLASSIFIED

SECURITY CLASSIFICATION OF THIS PAGE (When Data Entered)

REPORT DOCUMENTATION PAGE

READ INSTRUCTIONS BEFORE COMPLETING FORM

1. REPORT NUMBER: T-79-1
2. GOVT ACCESSION NO.
3. RECIPIENT'S CATALOG NUMBER
4. TITLE (and Subtitle): GYROCOMPASSING ERROR ANALYSIS FOR PERSHING II INERTIAL MEASUREMENT UNIT
5. TYPE OF REPORT & PERIOD COVERED: Technical Report
6. PERFORMING ORG. REPORT NUMBER
7. AUTHOR(s): H. V. White and J. C. Hung
8. CONTRACT OR GRANT NUMBER(s)
9. PERFORMING ORGANIZATION NAME AND ADDRESS: Commander, US Army Missile Research and Development Command, Attn: DRDMI-TG, Redstone Arsenal, Alabama 35809
10. PROGRAM ELEMENT, PROJECT, TASK AREA & WORK UNIT NUMBERS: DA N/A, AMCMS 643311.5990012
11. CONTROLLING OFFICE NAME AND ADDRESS: Commander, US Army Missile Research and Development Command, Attn: DRDMI-TI, Redstone Arsenal, Alabama 35809
12. REPORT DATE: November 1978
13. NUMBER OF PAGES: 39
14. MONITORING AGENCY NAME & ADDRESS (if different from Controlling Office)
15. SECURITY CLASS. (of this report): UNCLASSIFIED
15a. DECLASSIFICATION/DOWNGRADING SCHEDULE
16. DISTRIBUTION STATEMENT (of this Report): Approved for public release; distribution unlimited.
17. DISTRIBUTION STATEMENT (of the abstract entered in Block 20, if different from Report)
18. SUPPLEMENTARY NOTES
19. KEY WORDS (Continue on reverse side if necessary and identify by block number):
   - Sensor anomalies
   - Ground vibration
   - Measurement noise
20. ABSTRACT (Continue on reverse side if necessary and identify by block number):

This report documents the result of several error analyses for PERSHING II inertial measurement unit gyrocompassing. The analyses have been beneficial in three ways. They offered an opportunity for a better understanding of the underlying mechanisms governing the dependence of gyrocompassing error on error sources. The analytic results provide a means for estimating gyrocompassing error from known error sources, and pave the way for the development of a → next page

ABSTRACT (CONTINUED)

DD FORM 1 JAN 73 1473 EDITION OF 1 NOV 65 IS OBSOLETE

SECURITY CLASSIFICATION OF THIS PAGE (When Data Entered)

79 04 16 022

ABSTRACT (CONCLUDED)

cont.
technique for identifying source errors from a properly devised test. Three categories of error sources are discussed. Detailed analyses were made for two categories. Analysis for the third category was not ~~previously~~ done there by the authors and was documented in detail elsewhere.

CONTENTS

I. INTRODUCTION

Recently, the development of a new automatic gyrocompassing technique for Pershing II (PII), an improved version of the Pershing missile has been reported [1-11]. The goal is to have a faster and more accurate azimuth self-alignment with minimum effort from human operators. Among the reported subjects are a new gyrocompassing concept, the theoretical foundation, implementation scheme, methods of on-line data reduction, computation algorithms, programming considerations for software, laboratory test method and result evaluation, and techniques for field test and data reduction.

This report documents the result of several error analyses for PII inertial measurement unit (IMU) gyrocompassing performed during the course of gyrocompassing development. The analyses have been beneficial for the development as follows:

a) The process of analysis revealed more insight for understanding the underlying principles dictating the dependence of gyrocompassing error on various source errors.

b) The analysis yielded a formula for estimating gyrocompassing error from known source errors.

c) The analytic result obtained provides a background for developing techniques for identification of source errors using certain test data.

Gyrocompassing is performed on a gimballed IMU before missile launching. The operation amounts to establishing the initial alignment of the IMU platform coordinates with respect to a geodetic coordinate system. There are many error sources which effect gyrocompassing accuracy. Among them are sensor anomalies, ground vibrations, and measurement noise. Their effects will all be analyzed here. To make this report reasonably self contained, the gyrocompassing scheme used will first be reviewed.

The geodetic reference adopted is a triad (N,E,A) as shown in Figure 1 where three reference axes are pointed northward, eastward, and vertically downward. Ideally, the x, y, and z axes of the IMU's platform are in the downrange, right-hand crossrange, and downward directions, with x and y axes in the horizontal plane. Gyrocompassing is performed to determine the azimuth of the x axis measured with respect to the geodetic north.

II. THE GYROCOMPASSING SCHEME

The gyrocompassing scheme [1,5,7] adopted is referred to as "two-position offset zero-torquing gyrocompassing." In the schema, platform

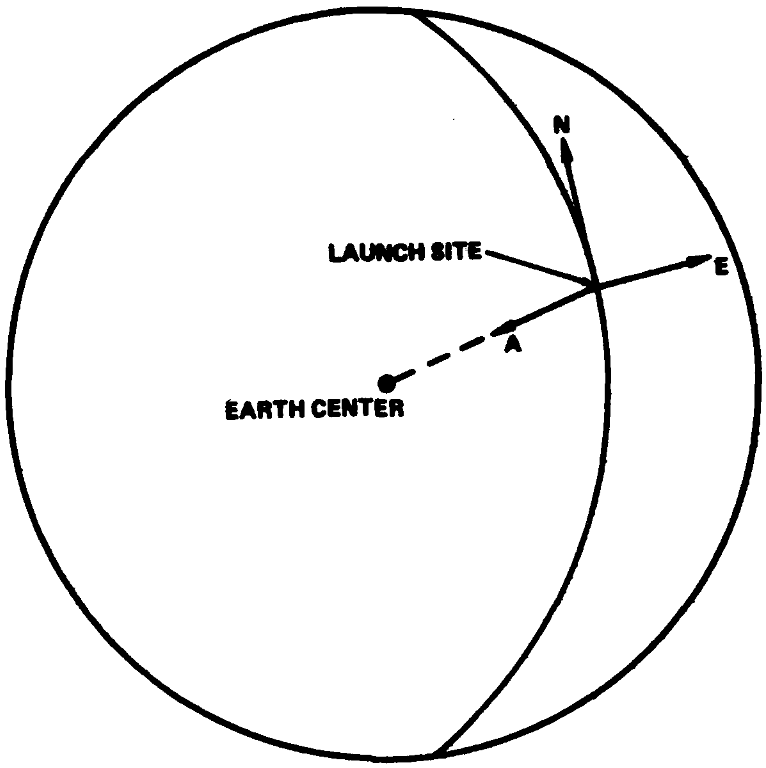

Figure 1. A geodetic reference frame.

fine alignment is done analytically for two platform positions which are 90° apart in the horizontal plane. Alignment in the first position is primarily for determining the drift of an equivalent north gyro which is a fictitious gyro representing the combined effects of x and y gyros in the north direction. This equivalent north gyro becomes an equivalent east gyro in the second position. Alignment data obtained in the second position together with the east gyro drift allow the determination of azimuth heading of the platform's x-axis. The word "offset" refers to the feature which permits gyrocompassing with the platform x-axis offset from north at any azimuth heading. Zero torquing refers to the concept of opening the leveling loops of the platform during data taking, thus reducing the effect of gyro torquer scale factor uncertainties. A summary of the gyrocompassing procedure is given in the following paragraphs.

Step 1: In the first position, the platform is approximately level, with its x-axis at any offset angle α with respect to north. A crude estimate of α is made using any best available true heading (BATH) technique.

Step 2: Both of the platform leveling loops are opened at outputs of two accelerometers, which removes the torquing of two level axes of the platform. Torquing of the vertical axis of the platform is maintained at a rate equal to the vertical component of earth rate. Outputs of x and y accelerometers, which are in the form of incremental velocities ΔV_x and ΔV_y, are measured.

Step 3: A rotational transformation on ΔV_x and ΔV_y is applied to give ΔV_N and ΔV_E, the equivalent incremental velocities in the north and east directions, respectively. The transformation is represented by

$$\Delta V_N = \Delta V_x \cos \alpha - \Delta V_y \sin \alpha \tag{1}$$

$$\Delta V_E = \Delta V_x \sin \alpha + \Delta V_y \cos \alpha \tag{2}$$

Step 4: By integrating accelerometer outputs, apparent north velocity V_N and east velocity V_E, caused by the tilt of platform, are obtained. They are related to platform parameters as follows:

$$V_N = \theta_{EO} t + 1/2\ D'_{EO} t^2 - 1/6\ D'_{NO}\ \Omega_A t^3 \tag{3}$$

$$V_E = -\theta_{NO} t - 1/2\ D'_{NO} t^2 - 1/6\ D'_{EO}\ \Omega_A t^3 \tag{4}$$

where the unit for velocity is in g-seconds and g is the gravitational acceleration.

In Equations (3) and (4), θ_{NO} and θ_{EO} are the initial misalignments of the platform about the north and east directions, respectively; D'_{NO} and D'_{EO} are initial platform drifts about north and east directions; Ω_A is the vertical component of earth rate Ω, and t is the time variable. V_N and V_E are obtained at 1250 instants during a 240-sec period, resulting in 2500 data pieces from which platform parameters are determined using one of two available least-square regression algorithms.

Step 5: A first azimuth misalignment ψ is computed using

$$\psi = \frac{D'_{NO}}{\Omega \cos L} - \theta_{NO} \tan L \quad , \tag{5}$$

and the north gyro drift D_N using

$$D_N = D'_{NO} - (1 - \cos \psi) - \theta_{EO} \Omega_A \quad . \tag{6}$$

In Equation (5), L is the latitude of launch site.

Step 6: Both leveling loops are closed and the IMU platform is slewed approximately 90° about its vertical axis so that the original platform-north becomes the new platform-east and the original platform-east becomes the new platform-south.

Step 7: Both leveling loops are opened again at outputs of x and y accelerometers. A new offset angle α is estimated by BATH for this second position. Repeat Steps 2, 3, and 4 for a new set of platform parameters.

Step 8: The refined initial azimuth misalignment angle θ_{AO} is computed using

$$\theta_{AO} = \frac{(D'_{EO})_2 - (D_N)_1}{\Omega \cos L} - (\theta_{NO})_2 \tan L \tag{7}$$

where $(\ )_1$ and $(\ )_2$ indicate results obtained at the first and second positions, respectively.

Step 9: The azimuth misalignment θ_{AO} is the finely determined angular correction for the crudely estimated offset angle α. Therefore, the initial azimuth heading, H_O, of the platform's x-axis can be computed from

$$H_O = \alpha + \theta_{AO} \quad . \tag{8}$$

The final result of gyrocompassing consists of accurately determined initial azimuth heading H_O, initial platform misalignment angles θ_{NO} and θ_{EO}, and initial drift coefficients D'_{NO} and D'_{EO}. These parameters will all be used for the initialization of the missile's navigation and guidance system.

III. ERROR SOURCES

Various error sources may be grouped into three different categories. The first category consists of all error sources which result in heading-sensitive gyrocompassing errors. These error sources are as follows:

a) Accelerometer scale factor uncertainties K_x, K_y, and K_z.

b) The fixed part of accelerometer bias uncertainties B_x, B_y, B_z and the variable part ΔB_x, ΔB_y, ΔB_z representing the differences of accelerometer biases at the first and second gyrocompassing positions.

c) Gyro heading-sensitive drift uncertainties H_{sx}, H_{sy}, H_{sz}.

d) Y-accelerometer non-orthogonality δ_{xy} which is in the xy-plane.

e) Gyro input-axis g-sensitive drift uncertainties D_{Ix} and D_{Iy}.

f) Gyro spin-axis sensitive drift uncertainties $D_{\delta x}$ and $D_{\delta y}$.

g) Gravity uncertainty ε_g.

h) Latitude uncertainty ε_L.

The subscripts x, y, and z denote the respective platform axes to which sensors are associated. Error sources in this category are assumed stationary during a short time period, for example, one hour. It should be noted that all known anomalies are not considered errors because their effect can be compensated by software during data processing.

The second category consists of all sources which cause base motion. These sources include ground vibrations and wind gusts which are, in general, time-varying.

The third category of error sources includes measurement noise which may be considered as independent white noise. Gyrocompassing error due to measurement noise has been analyzed and recently reported by the authors [1,3,7]. Therefore, this case will not be discussed further in this report.

IV. HEADING SENSITIVE ERRORS

A. Accelerometer Outputs

Three rectangular coordinate frames will be used as follows:

1) The geodetic frame with axes N, E, and A as shown in Figure 1.

2) The ideal platform frame with axes X, Y, and Z which are pointed in the downrange, right-hand crossrange, and vertically downward directions.

3) The actual platform frame x, y, and z which is misaligned from X, Y, and Z respectively.

The misalignment of the platform is represented by three Euler angles θ_x, θ_y, and θ_z rotated about the x, y, and z axes, respectively, in that order.

The transformation between (N,E,A) and (X,Y,Z) for an offset angle α, as shown in Figure 2, is given by

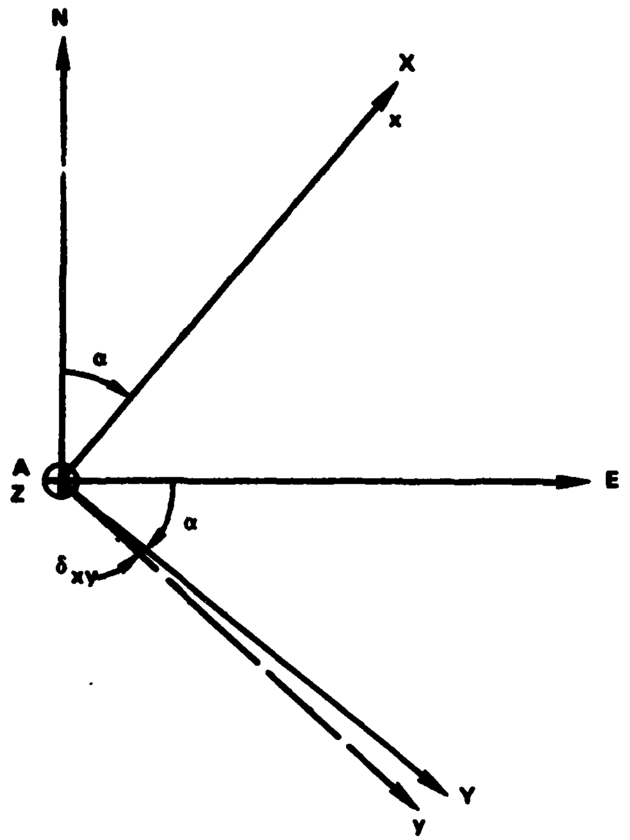

Figure 2. Offset α and non-orthogonality δ_{xy}.

$$\begin{bmatrix} X \\ Y \\ Z \end{bmatrix} = T_1 \begin{bmatrix} N \\ E \\ A \end{bmatrix} \tag{9}$$

where

$$T_1 = \begin{bmatrix} \cos\alpha & \sin\alpha & 0 \\ -\sin\alpha & \cos\alpha & 0 \\ 0 & 0 & 1 \end{bmatrix} . \tag{10}$$

Transformation from the ideal platform frame (X,Y,Z) to the actual platform frame (x,y,z) represents the effect of misalignment angles θ_x, θ_y, θ_z, and the non-orthogonality angle δ_{xy} as shown in Figure 2. They are

$$\begin{bmatrix} X \\ Y \\ Z \end{bmatrix} = T_3\, T_2 \begin{bmatrix} X \\ Y \\ Z \end{bmatrix} \tag{11}$$

where

$$T_2 = \begin{bmatrix} C\theta_z & S\theta_z & 0 \\ -S\theta_z & C\theta_z & 0 \\ 0 & 0 & 1 \end{bmatrix} \begin{bmatrix} C\theta_y & 0 & -S\theta_y \\ 0 & 1 & 0 \\ S\theta_y & 0 & C\theta_y \end{bmatrix} \begin{bmatrix} 1 & 0 & 0 \\ 0 & C\theta_x & S\theta_x \\ 1 & -S\theta_x & C\theta_x \end{bmatrix}$$

$$= \begin{bmatrix} C\theta_y\, C\theta_z & S\theta_x\, S\theta_y\, C\theta_z + C\theta_x\, S\theta_z & -C\theta_x\, S\theta_y\, C\theta_z + S\theta_x\, S\theta_z \\ -C\theta_y\, S\theta_z & -S\theta_x\, S\theta_y\, S\theta_z + C\theta_x\, C\theta_z & C\theta_x\, S\theta_y\, S\theta_z + S\theta_x\, C\theta_z \\ S\theta_y & -S\theta_x\, C\theta_y & C\theta_x\, C\theta_y \end{bmatrix} \tag{12}$$

and

$$T_3 = \begin{bmatrix} 1 & 0 & 0 \\ -S\delta_{xy} & C\delta_{xy} & 0 \\ 0 & 0 & 1 \end{bmatrix} . \tag{13}$$

The notations $C\theta = \cos\theta$ and $S\theta = \sin\theta$ are used to save space.

During prelaunch gyrocompassing, the missile is stationary, and in the absence of base vibratory inputs, all acceleration components are due to the earth's gravitational acceleration g. The measured accelerations along (x,y,z) frame are given by

$$\begin{bmatrix} a_x \\ a_y \\ a_z \end{bmatrix} = T_3\, T_2\, T_1 \begin{bmatrix} a_N \\ a_E \\ a_A \end{bmatrix} \tag{14}$$

where

$$\begin{bmatrix} a_N \\ a_E \\ a_A \end{bmatrix} = \begin{bmatrix} 0 \\ 0 \\ -1 \end{bmatrix} . \tag{15}$$

The unit for acceleration is the number of g's.

By modifying Equations (14) and (15), effects of accelerometer scale factor uncertainties, accelerometer bias uncertainties, and gravity uncertainty can be taken into account. Let K be a scale factor matrix; that is

$$K = \begin{bmatrix} K_x & 0 & 0 \\ 0 & K_y & 0 \\ 0 & 0 & K_z \end{bmatrix} \quad . \tag{16}$$

Considering the previously mentioned uncertainties, Equations (14) and (15) give

$$\begin{bmatrix} a_x \\ a_y \\ a_z \end{bmatrix} = [I + K]\ T \begin{bmatrix} 0 \\ 0 \\ -1-\varepsilon_g \end{bmatrix} + \begin{bmatrix} B_x \\ B_y \\ B_z \end{bmatrix} \tag{17}$$

where

$$T = T_3\ T_2\ T_1 \quad . \tag{18}$$

The bias uncertainties have the same unit as acceleration, which is the number of g's.

Equation (17), with its exact details, is rather complex and hard to analyze. Fortunately, in practice, angular misalignments are sufficiently small so that small angle approximations are valid, namely, $\cos\theta \simeq 1$ and $\sin\theta \simeq \theta$. Applying the approximation to angles θ_x, θ_y, θ_z, and δ_{xy} in Equation (18) and neglecting second and higher order terms result in

$$T = \begin{bmatrix} 1 & 0 & 0 \\ -\delta_{xy} & 1 & 0 \\ 0 & 0 & 1 \end{bmatrix} \begin{bmatrix} 1 & \theta_z & -\theta_y \\ -\theta_z & 1 & \theta_x \\ \theta_y & \theta_x & 1 \end{bmatrix} \begin{bmatrix} C\alpha & S\alpha & 0 \\ -S\alpha & C\alpha & 0 \\ 0 & 0 & 1 \end{bmatrix}$$

$$= \begin{bmatrix} C\alpha - \theta_z S\alpha & S\alpha + \theta_z C\alpha & -\theta_y \\ -S\alpha - \theta_z C\alpha - \delta_{xy} C\alpha & C\alpha - \theta_z S\alpha - \delta_{xy} S\alpha & \theta_x \\ \theta_y C\alpha + \theta_x S\alpha & \theta_y S\alpha - \theta_x C\alpha & 1 \end{bmatrix} \quad . \tag{19}$$

Substituting Equation (19) into Equation (17) and expressing the result in expanded form yield

$$\begin{bmatrix} a_x \\ a_y \\ a_z \end{bmatrix} = \begin{bmatrix} (1 + K_x)\ \theta_y\ (1 + \varepsilon_g) \\ (1 + K_y)\ \theta_x\ (-1 - \varepsilon_g) \\ (1 + K_z)\ (-1 - \varepsilon_g) \end{bmatrix} + \begin{bmatrix} B_x \\ B_y \\ B_z \end{bmatrix} \quad . \tag{20}$$

The third order variations $K_y \theta_x \varepsilon_g$ and $K_x \theta_y \varepsilon_g$ in Equation (20) are neglected

$$\left.\begin{aligned} a_x &= (1 + K_x + \varepsilon_g)\ \theta_y + B_x \\ a_y &= -(1 + K_y + \varepsilon_g)\ \theta_x + B_y \\ a_z &= -(1 + K_z + \varepsilon_g) + B_z \end{aligned}\right\} \quad . \tag{21}$$

By examining Equation (21), it is seen that δ_{xy}, the y-axis non-orthogonality, is absent. The reason is that the effect of δ_{xy} on accelerometer outputs is second order in nature. Physically, if the platform has no misalignment, δ_{xy} has no effect on accelerometer outputs during gyrocompassing.

It is desirable to retain δ_{xy} in the model for accelerometer outputs so that its effect on gyrocompassing can be monitored. Instead of dropping all second and higher order terms in obtaining Equation (19), those second order terms containing δ_{xy} will be retained. Therefore, Equation (18) gives

$$T = \begin{bmatrix} C\alpha - \theta_z S\alpha & S\alpha + \theta_z C\alpha & -\theta_y \\ -S\alpha - \theta_z C\alpha + \delta_{xy} (\theta_z S\alpha - C\alpha) & C\alpha - \theta_z S\alpha - \delta_{xy} (\theta_z C\alpha + S\alpha) & \theta_y \delta_{xy} + \theta_x \\ \theta_y C\alpha + \theta_x S\alpha & \theta_y S\alpha - \theta_x C\alpha & 1 \end{bmatrix} \quad . \tag{22}$$

The desired expression for accelerometer outputs is obtained by substituting Equation (22) into Equation (17).

$$\left.\begin{aligned} a_x &= (1 + K_y + \varepsilon_g)\ \theta_y + B_x \\ a_y &= -(1 + K_y + \varepsilon_g)\ (\theta_x + \theta_y \delta_{xy}) + B_y \\ a_z &= -(1 + K_z + \varepsilon_g) + B_z \end{aligned}\right\} \quad . \tag{23}$$

The effect of δ_{xy} appears only in the y-acceleration. This effect vanishes when the platform is level. The outputs of accelerometers are time-varying because misalignments are changing due to platform drift. The dynamic property of the platform will be analyzed next.

B. Drift Dynamics of the Platform

The platform of a gimballed IMU is tightly slaved to its gyros; therefore, gyro drifts completely appear as part of the platform drift. Let D'_x, D'_y and D'_z denote drifts of the platform about its x, y, and z axes, respectively. When leveling loops of the platform are open, the drift of the platform consists of not only gyro drifts, but also earth rotation and the effect of platform misalignment; therefore,

$$\begin{bmatrix} D'_x \\ D'_y \\ D'_z \end{bmatrix} = \begin{bmatrix} D_x \\ D_y \\ D_z \end{bmatrix} - T_2 \; T_1 \begin{bmatrix} \Omega_N \\ 0 \\ \Omega_A \end{bmatrix} \tag{24}$$

where $\Omega_N = \Omega \cos L$ and $\Omega_A = -\Omega \sin L$. The first right-hand term of this equation represents gyro drifts; the second term represents the combined effect of earth rotation and platform misalignment. The transformation T_2 in Equation (24) is given by

$$T_2 = \begin{bmatrix} 1 & \theta_z & -\theta_y \\ -\theta_z & 1 & \theta_x \\ \theta_y & -\theta_x & 1 \end{bmatrix} \tag{25}$$

which is obtained by applying small angle approximations to Equation (12).

It is noted that

$$\left.\begin{aligned} \theta_x &= \theta_{xo} + \int_o^t D'_x(t)\,dt \\ \theta_y &= \theta_{yo} + \int_o^t D'_y(t)\,dt \\ \theta_z &= \theta_{zo} + \int_o^t D'_z(t)\,dt \end{aligned}\right\} \tag{26}$$

where the subscript "o" implies initial value. Using Equation (26) in Equation (25) and substituting the result into Equation (24) give

$$\left.\begin{aligned} D'_x &= D'_{xo} + \Omega_N S\alpha \int_o^t D'_z\, dt + \Omega_A \int_o^t D'_y\, dt \\ D'_y &= D'_{yo} + \Omega_N C\alpha \int_o^t D'_z\, dt - \Omega_A \int_o^t D'_x\, dt \\ D'_z &= D'_{zo} - \Omega_N S\alpha \int_o^t D'_x\, dt - \Omega_N C\alpha \int_o^t D'_y\, dt \end{aligned}\right\} \tag{27}$$

where

$$D'_{xo} = D_x - C\alpha\, \Omega_N + \theta_{zo}\, \Omega_N\, S\alpha + \theta_{yo}\, \Omega_A \tag{28a}$$

$$D'_{yo} = D_y + S\alpha\, \Omega_N + \theta_{zo}\, \Omega_N\, C\alpha - \theta_{xo}\, \Omega_A \tag{28b}$$

$$D'_{zo} = D_z - \Omega_A - \theta_{yo}\, \Omega_N\, C\alpha - \theta_{xo}\, \Omega_N\, S\alpha \tag{28c}$$

are initial values for D'_x, D'_y, and D'_z.

Taking the Laplace transform of Equation (27) and expressing the result in matrix form, result in

$$\begin{bmatrix} s\, D'_x\ (s) \\ s\, D'_y\ (s) \\ s\, D'_z\ (s) \end{bmatrix} = E \begin{bmatrix} D'_x\ (s) \\ D'_y\ (s) \\ D'_z\ (s) \end{bmatrix} \tag{29}$$

where

$$E = \begin{bmatrix} 0 & \Omega_A & \Omega_N\, S\alpha \\ -\Omega_A & 0 & \Omega_N\, C\alpha \\ -\Omega_N\, S\alpha & -\Omega_N\, C\alpha & 0 \end{bmatrix} \quad . \tag{30}$$

The characteristic polynominal of Equation (29) is

$$|sI - E| = s^3 + \left(\Omega_A^2 + \Omega_N^2\right) s = s(s^2 + \Omega^2) \quad . \tag{31}$$

The solution for Equation (29) is

$$\begin{bmatrix} D'_x\ (s) \\ D'_y\ (s) \\ D'_z\ (s) \end{bmatrix} = [sI - E]^{-1} \begin{bmatrix} D'_{xo} \\ D'_{yo} \\ D'_{zo} \end{bmatrix} \quad . \tag{32}$$

In the expanded form.

$$\begin{aligned} D'_x\ (s) = D'_{xo} & \left[\frac{C^2L\ C^2\alpha}{s} + \frac{(1 - C^2L\ C^2\alpha)s}{s^2 + \Omega^2}\right] \\ + D'_{yo} & \left[\frac{C^2L\ C\alpha\ S\alpha\ s + \Omega_A}{s^2 + \Omega^2} - \frac{C^2L\ C\alpha\ S\alpha}{s}\right] \\ + D'_{zo} & \left[\frac{CL\ SL\ C\alpha}{s} - \frac{CL\ SL\ C\alpha\ s + \Omega_N\ S\alpha}{S^2 + \Omega^2}\right] \end{aligned} \tag{33}$$

$$\begin{aligned} D'_y\ (s) = D'_{xo} & \left[\frac{C^2L\ C\alpha\ S\alpha\ s - \Omega_A}{s^2 + \Omega^2} - \frac{C^2L\ C\alpha\ S\alpha}{s}\right] \\ + D'_{yo} & \left[\frac{C^2L\ S^2\alpha}{s} + \frac{(1 - C^2L\ S^2\alpha)s}{s^2 + \Omega^2}\right] \\ + D'_{zo} & \left[\frac{CL\ SL\ S\alpha\ s + \Omega_N\ C\alpha}{s^2 + \Omega^2} - \frac{CL\ SL\ S\alpha}{s}\right] \end{aligned} \tag{34}$$

$$\begin{aligned} D'_z\ (s) = D'_{xo} & \left[\frac{CL\ SL\ C\alpha}{s} - \frac{CL\ SL\ C\alpha + \Omega_N\ S\alpha}{s^2 + \Omega^2}\right] \\ + D'_{yo} & \left[\frac{CL\ SL\ S\alpha\ s - \Omega_N\ C\alpha}{s^2 + \Omega^2} - \frac{CL\ SL\ S\alpha}{s}\right] \\ + D'_{zo} & \left[\frac{S^2L}{s} + \frac{(1 - S^2L)s}{s^2 + \Omega^2}\right] \quad . \end{aligned} \tag{35}$$

By taking the inverse Laplace transform of Equations (33), (34), and (35), time response of drifts is obtained as follows:

$$
\begin{aligned}
D'_x(t) = {} & [C^2L\ C^2\alpha + (1 - C^2L\ C^2\alpha)\ C(\Omega t)]\ D'_{xo} \\
& + [C^2L\ C\alpha\ S\alpha\ C(\Omega t) + SL\ S(\Omega t) - C^2L\ C\alpha\ S\alpha]\ D'_{yo} \\
& + [CL\ SL\ C\alpha - CL\ SL\ C\alpha\ C(\Omega t) - CL\ S\alpha\ S(\Omega t)]\ D'_{zo}
\end{aligned} \tag{36}
$$

$$
\begin{aligned}
D'_y(t) = {} & [C^2L\ C\alpha\ S\alpha\ C\ (\Omega t) - SL\ C(\Omega t) - C^2L\ C\alpha\ S\alpha]\ D'_{xo} \\
& + [C^2L\ S^2\alpha + (1 - C^2L\ S^2\alpha)\ C(\Omega t)]\ D'_{yo} \\
& + [CL\ SL\ S\alpha\ C(\Omega t) + CL\ C\alpha\ S(\Omega t) - CL\ SL\ S\alpha]\ D'_{zo}
\end{aligned} \tag{37}
$$

$$
\begin{aligned}
D'_z(t) = {} & [CL\ SL\ C\alpha - CL\ SL\ C\alpha\ C(\Omega t) - CL\ S\alpha\ S(\Omega t)]\ D'_{xo} \\
& + [CL\ SL\ S\alpha\ C(\Omega t) - CL\ C\alpha\ S(\Omega t) - CL\ SL\ S\alpha]\ D'_{yo} \\
& + [S^2L + (1 - S^2L)\ C(\Omega t)]\ D'_{zo} \quad .
\end{aligned} \tag{38}
$$

The data taking period for gyrocompassing is sufficiently short so that $C(\Omega t) \approx 1$ and $S(\Omega t) \approx \Omega t$. Therefore, Equations (36), (37), and (38) can be adequately approximated by

$$
\left.
\begin{aligned}
D'_x(t) &= D'_{xo} + D'_{yo}\ \Omega_A t + D'_{zo}\ S\alpha\ \Omega_N t \\
D'_y(t) &= D'_{yo} - D'_{xo}\ \Omega_A t + D'_{zo}\ C\alpha\ \Omega_N t \\
D'_z(t) &= D'_{zo} - D'_{xo}\ S\alpha\ \Omega_N t - D'_{yo}\ C\alpha\ \Omega_N t
\end{aligned}
\right\} \quad . \tag{39}
$$

By integrating Equation (39) the time response of platform misalignment is obtained:

$$
\left.
\begin{aligned}
\theta_x(t) &= \theta_{xo} + D'_{xo} t + \frac{t^2}{2}\ (D'_{yo}\ \Omega_A + D'_{zo}\ S\alpha\ \Omega_N) \\
\theta_y(t) &= \theta_{yo} + D'_{yo} t + \frac{t^2}{2}\ (D'_{zo}\ C\alpha\ \Omega_N - D'_{xo}\ \Omega_A) \\
\theta_z(t) &= \theta_{zo} + D'_{zo} t - \frac{t^2}{2}\ (D'_{xo}\ S\alpha\ \Omega_N + D'_{yo}\ C\alpha\ \Omega_N)
\end{aligned}
\right\} \quad . \tag{40}
$$

C. Errors in Velocity

Substituting Equation (40) into Equation (23) gives accelerometer outputs which contain K_x, K_y, K_z, B_x, B_y, B_z, ε_g, and δ_{xy} as follows:

$$a_x = (1 + K_x + \varepsilon_g) \left[\theta_{yo} + D'_{yo} t + \frac{t^2}{2} (D'_{zo} \, C\alpha \, \Omega_N - D'_{xo} \, \Omega_A)\right] + B_x \quad (41)$$

$$\begin{aligned} a_y = & -(1 + K_y + \varepsilon_g) \Big[(\theta_{xo} + \theta_{yo} \, \delta_{xy}) + (D'_{xo} + D'_{yo} \, \delta_{xy}) t \\ & + \frac{t^2}{2} (D'_{yo} \, \Omega_A + D'_{zo} \, S\alpha \, \Omega_N + D'_{zo} \, C\alpha \, \Omega_N \, \delta_{xy} - D'_{xo} \, \Omega_A \, \delta_{xy})\Big] \\ & + B_y \end{aligned} \quad (42)$$

$$a_z = -(1 + K_z + \varepsilon_g) + B_z \quad . \quad (43)$$

The velocity is obtained by integrating Equations (41), (42), and (43) as follows:

$$\begin{aligned} V_x = & \left[B_x + (1 + K_x + \varepsilon_g) \, \theta_{yo}\right] t + \left[(1 + K_x + \varepsilon_g) \, D'_{yo}\right] \frac{t^2}{2} \\ & + \left[(1 + K_x + \varepsilon_g) (D'_{zo} \, C\alpha \, \Omega_N - D'_{xo} \, \Omega_A)\right] \frac{t^3}{6} \end{aligned} \quad (44)$$

$$\begin{aligned} V_y = & \left[B_y - (1 + K_y + \varepsilon_g) (\theta_{xo} + \theta_{yo} \, \delta_{xy})\right] t \\ & - \left[(1 + K_y + \varepsilon_g) (D'_{xo} + D'_{yo} \, \delta_{xy})\right] \frac{t^2}{2} \\ & - \Big[(1 + K_y + \varepsilon_g) (D'_{yo} \, \Omega_A + D'_{zo} \, S\alpha \, \Omega_N + D'_{zo} \, C\alpha \, \Omega_N \, \delta_{xy} \\ & - D'_{xo} \, \Omega_A \, \delta_{xy})\Big] \frac{t^3}{6} \end{aligned} \quad (45)$$

$$V_z = \left[B_z - (g + K_z + \varepsilon_g)\right] t \quad . \quad (46)$$

Equations (44), (45), and (46) give velocities along three platform axes. The velocities derived from a set of equivalent platform north and east accelerometers can be obtained from Equations (44) and (45) via a coordinate transformation. They are

$$V_N = V_x C\alpha - V_y S\alpha$$

$$= C\alpha \left\{\left[B_x + (1 + K_x + \varepsilon_g)\ \theta_{yc}\right]t + \left[(1 + K_x + \varepsilon_g)\ D'_{yo}\right]\right\} \frac{t^2}{2}$$

$$+ \left[(1 + K_x + \varepsilon_g)\ (D'_{zo}\ C\alpha\ \Omega_N - D'_{xo}\ \Omega_A)\right]\frac{t^3}{6}\Bigg\}$$

$$- S\alpha\ \left[B_y - (1 + K_y + \varepsilon_g)\ (\theta_{xo} + \theta_{yo}\ \delta_{xy})\right] t$$

$$- \left[(1 + K_y + \varepsilon_g)\ (D'_{xo} + D'_{yo}\ \delta_{xy})\right] \frac{t^2}{2}$$

$$- \left[(1 + K_y\ \varepsilon_g)\ (D'_{yo}\ \Omega_A + D'_{zo}\ S\alpha\ \Omega_N + D'_{zo}\ C\alpha\ \Omega_N\ \delta_{xy}\right.$$

$$\left. - D'_{xo}\ \Omega_A\ \delta_{xy})\right]\frac{t^3}{6}\Bigg\} \tag{47}$$

$$V_E = V_x\ S\alpha + V_y\ C\alpha$$

$$= S\alpha \left\{\left[B_x + (1 + K_x + \varepsilon_g)\ \theta_{yo}\right]\ t + \left[(1 + K_x + \varepsilon_g)\ D'_{yo}\right]\frac{t^2}{2}\right.$$

$$+ \left[(1 + K_x + \varepsilon_g)\ (D'_{zo}\ C\alpha\ \Omega_N - D'_{xo}\ \Omega_A)\right]\ \frac{t^3}{6}\Bigg\}$$

$$+ C\alpha\ \left[B_y - (1 + K_y + \varepsilon g)\ (\theta_{xo} + \theta_{yo}\ \delta_{xy})\right] t$$

$$- \left[(1 + K_y + \varepsilon_g)\ (D'_{xo} + D'_{yo}\ \delta_{xy})\right]\ \frac{t^2}{2}$$

$$- \left[(1 + K_y + \varepsilon_g)\ (D'_{yo}\ \Omega_A + D'_{zo}\ S\alpha\ \Omega_N + D'_{zo}\ C\alpha\ \Omega_N\ \delta_{xy}\right.$$

$$\left. - D'_{xo}\ \Omega_A\ \delta_{xy})\right]\ \frac{t^3}{6}\Bigg\}\ . \tag{48}$$

The error-free north and east velocity can be obtained from Equations (47) and (48) by nulling K_x, K_y, B_x, B_y, ε_g, and δ_{xy}. In addition, D'_{zo} is set to zero, since this is one of the assumptions under which gyrocompassing Equation (7) is derived. Denoting error-free velocities by superscript "0", the following is obtained:

$$V_N{}^0 = C\alpha\left\{\theta_{yo}t + D'_{yo}\frac{t^2}{2} - D'_{xo}\,\Omega_A\,\frac{t^3}{6}\right\}$$
$$+ S\alpha\left\{\theta_{xo}t + D'_{xo}\frac{t^2}{2} + D'_{yo}\,\Omega_A\,\frac{t^3}{6}\right\}$$
$$= \left\{\theta_{EO}t + D'_{EO}\frac{t^2}{2} - D'_{NO}\,\Omega_A\,\frac{t^3}{6}\right\} \tag{49}$$

$$V_E{}^0 = S\alpha\left\{\theta_{yo}t + D'_{yo}\frac{t^2}{2} - D'_{xo}\,\Omega_A\,\frac{t^3}{6}\right\}$$
$$+ C\alpha\left\{-\theta_{xo}t - D'_{xo}\frac{t^2}{2} - D'_{yo}\,\Omega_A\,\frac{t^3}{6}\right\}$$
$$= \left\{-\theta_{NO}t - D'_{NO}\frac{t^2}{2} - D'_{EO}\,\Omega_A\,\frac{t^3}{6}\right\} \tag{50}$$

where

$$\theta_{NO} = \theta_{xo}\,C\alpha - \theta_{yo}\,S\alpha \tag{51}$$
$$\theta_{EO} = \theta_{xo}\,S\alpha + \theta_{yo}\,C\alpha \tag{52}$$
$$D'_{NO} = D'_{xo}\,C\alpha - D'_{yo}\,S\alpha \tag{53}$$
$$D'_{EO} = D'_{xo}\,S\alpha + D'_{yo}\,C\alpha \quad . \tag{54}$$

Equations (49) and (50) are in fact Equations (3) and (4), respectively.

Expressions for velocity error ΔV_N and ΔV_E are obtained by subtracting $V_N{}^0$ from V_N and $V_E{}^0$ from V_E using Equations (47) through (50) as follows:

$$\Delta V_N = \left[B_x\,C\alpha - B_y\,S\alpha\right]t + \left[(K_x - K_y)\,\Omega_N\,S\alpha\,C\alpha + \Omega_N\,S^2\alpha\,\delta_{xy}\right]\frac{t^2}{2}$$
$$+ \left[D_z - \theta_{xo}\,\Omega_N\,S\alpha - \theta_{yo}\,\Omega_N\,C\alpha\right]\Omega_N\,\frac{t^3}{6} \tag{55}$$
$$\Delta V_E = \left[B_x\,S\alpha + B_y\,C\alpha\right]t$$
$$+ \left[K_x\,\Omega_N\,S^2\alpha + K_y\,\Omega_N\,C^2\alpha + \varepsilon_g\,\Omega_N - \Omega_N\,S\alpha\,C\alpha\,\delta_{xy}\right]\frac{t^2}{2} \quad . \tag{56}$$

The last bracketed term of Equation (55) comes from D'_{EO} using the relationship of Equation (28c) but with known quantity Ω_A deleted. Comparing Equations (55) and (56) to Equations (3) and (4), it can be seen that errors in the determination of θ_{NO}, θ_{EO}, D'_{NO}, and D'_{EO} are given by

$$\Delta\theta_{NO} = -(B_x\ S\alpha\ B_y\ C\alpha) = -B_E \tag{57}$$

$$\Delta\theta_{EO} = B_x\ C\alpha - B_y\ S\alpha = B_N \tag{58}$$

$$\Delta D'_{NO} = \delta_{xy}\ \Omega_N\ S\alpha\ C\alpha - K_x\ \Omega_N\ S^2\alpha - K_y\ \Omega_N\ C^2\alpha - \epsilon_g\ \Omega_N \tag{59}$$

$$\Delta D'_{EO} = \delta_{xy}\ \Omega_N\ S^2\alpha + (K_x - K_y)\ \Omega_N\ S\alpha\ C\alpha \quad . \tag{60}$$

D. Effect of Heading-Sensitive Gyro Drift

The heading-sensitive drifts for x and y gyros are designated H_{sy} and H_{sx}, respectively. Drifts for a set of equivalent north and east gyros are

$$H_{SN} = H_{sx} C\alpha - H_{sy} S_\alpha \tag{61}$$

$$H_{SE} = H_{sx} S\alpha + H_{sy} C\alpha \quad . \tag{62}$$

In the first platform position of gyrocompassing, the determined drift $(D_N)_1$ of the equivalent north gyro also contains the heading-sensitive drift $(H_{SN})_1$ and the two cannot be separated. This $(D_N)_1$ becomes $(D_E)_2$ at the second platform position. Because of the heading-sensitivity, $(H_{SE})_2$ is not equal to $(H_{SN})_1$ although both are referred to the same physical axis of the platform. The difference of $(H_{SE})_2$ and $(H_{SN})_1$ is contained in the determined $(D'_E)_2$ at the second position and is not readily separable from the latter. Fortunately, separation of $(H_{SN})_1$ from $(D_N)_1$ and of $(H_{SE})_2$ from $(D'_E)_2$ is not necessary. It is the relative value rather than the absolute value of the heading-sensitive drift which will be used in the gyrocompassing error analysis. Therefore, Equation (61) can be ignored but Equation (62) should be included in Equation (60) to give the error in the determined east-axis drift of the platform as

$$\begin{aligned} \Delta D'_{EO} &= \delta_{xy}\ \Omega_N\ S^2\alpha + (K_x - K_y)\ \Omega_N\ S\alpha\ C\alpha + H_{SE} \\ &= \delta_{xy}\ \Omega_N\ S^2\alpha + (K_x - K_y)\ \Omega_N\ S\alpha\ C\alpha + H_{sx}\ S\alpha + H_{sy}\ C\alpha \quad , \end{aligned} \tag{63}$$

E. Effect of Gyro Input-Axis g-Sensitive Drifts

The PII IMU employs a tuned-rotor type, two-degree-of-freedom gyro, for sensing attitude rate about the platform's x and y axes. From the physical consideration of the device, it is recognized that the coefficients of two input-axis g-sensitive drifts, D_{Ix} and D_{Iy}, are equal. Hence, both of them will be denoted by D_{Ixy}. During gyrocompassing, the equivalent north axis of the platform has little tilting motion, while the equivalent east axis is tilting appreciably due to the north component of earth rotation. The tilt of the east axis causes appreciable g-sensitive drift for an apparent east gyro, represented by the coefficient

$$D_{IE} = D_{Ix} S\alpha + D_{Iy} C\alpha = D_{Ixy} (S\alpha + C\alpha) \quad . \tag{64}$$

The unit for all D_I coefficients is degrees per hour per meter per second-squared $[(\mathrm{deg/hr})/(\mathrm{m/sec}^2)]$.

The tilt angle for the platform's east axis has a nominal value of $\Omega_N t$ when leveling loops are open. The average drift over a time interval T, the data taking period, is

$$\Delta_{IE} = \frac{1}{T} \int_0^T D_{IE}\, g\, \Omega_N t\, dt = \frac{1}{2} D_{IE}\, g\, \Omega_N T \quad . \tag{65}$$

This drift should also be included as part of the error of the determined east axis drift of the platform at the second platform position. This is done by including Equation (65) in Equation (63) giving

$$\begin{aligned} \Delta D'_{EO} = {} & \delta_{xy} \Omega_N S^2\alpha + (K_x - K_y) \Omega_N S\alpha C\alpha \\ & + H_{sx} S\alpha + H_{sy} C\alpha + \frac{1}{2} D_{Ixy} (S\alpha + C\alpha)\, g\, \Omega_N T \end{aligned} \tag{66}$$

where Equation (64) has been used to express D_{IE} in terms of D_{Ixy}.

F. Effect of Gyro Spin-Axis g-Sensitive Drifts

The effect of spin-axis g-sensitive drifts about the platform's x and y axes can be analyzed similarly. For the PII IMU, the spin-axis of level gyro is oriented vertically and experiences an acceleration of 1 g. The effect of the slight tilt of the vertical axis may be ignored because of the insensitivity of the cosine function near null. The characteristics of the spin-axis g-sensitive drifts about the x and y axes are represented by coefficients D_{sx} and D_{sy}. The equivalent coefficients for the platform's north and east axes are given by

$$D_{SN} = D_{sx}\ C\alpha - D_{sy}\ S\alpha \tag{67}$$

$$D_{SE} = D_{sx}\ S\alpha + D_{sy}\ C\alpha \quad . \tag{68}$$

The unit for all D_δ coefficients is degrees per hour per meter per second-squared. The drifts themselves are given by

$$\Delta_{SN} = g\ D_{SN} = g(D_{sx}\ C\alpha - D_{sy}\ S\alpha) \tag{69}$$

$$\Delta_{SE} = g\ D_{SE} = g(D_{sz}\ S\alpha + D_{sy}\ C\alpha) \tag{70}$$

for the north and east axes.

The effect of Δ_{SN} and Δ_{SE} can be accounted for by including them in Equations (59) and (66), respectively, which are errors of the determined north and east axis drifts. Therefore the following is obtained:

$$\begin{aligned} \Delta D'_{NO} = {} & \delta_{xy}\ \Omega_N\ S\alpha\ C\alpha - K_x\ \Omega_N\ S^2\alpha - K_y\ \Omega_N\ C^2\alpha \\ & - \varepsilon_g\ \Omega_N + g(D_{sx}\ C\alpha - D_{sy}\ S\alpha) \end{aligned} \tag{71}$$

$$\begin{aligned} \Delta D'_{EO} = {} & \delta_{xy}\ \Omega_N\ S^2\alpha + (K_x - K_y)\ \Omega_N\ S\alpha\ C\alpha + H_{sx}\ S\alpha + H_{sy}\ C\alpha \\ & + 1/2\ D_{Ixy}\ (S\alpha + C\alpha)\ g\ \Omega_N T + g(D_{sx}\ S\alpha + D_{sy}\ C\alpha) \quad . \end{aligned} \tag{72}$$

In Equation (72), the last two terms depend on the heading in the same way. The two cannot be separated by a multiple heading test. This conclusion will be discussed later.

G. Effect of Latitude Uncertainty

The effect of latitude uncertainty on gyrocompassing can be revealed by recalling Equation (7), the gyrocompassing equation,

$$\theta_{AO} = \frac{(D'_{EO})_2 - (\bar{D}_N)_1}{\Omega \cos L} - (\theta_{NO})_2 \tan L \quad .$$

The perturbation of this equation with respect to the latitude variation ε_L gives

$$\Delta\theta_{AO} = \frac{[(\Delta D'_{EO})_2 - (\Delta D_N)_1]\ \Omega\ CL + [(D'_{EO})_2 - (D_N)_1]\ \Omega\ SL\ \epsilon_L}{\Omega^2\ C^2 L}$$

$$- \Delta\theta_{NO} \tan L - \theta_{NO} \sec^2 L\ \epsilon_L \tag{73}$$

Using Equations (6), (53), (28a), and (28b), the variation $\Delta(D_N)_1$ can be obtained as follows:

$$(\Delta D_{N1}) = (\Delta D'_{NO})_1 = \Delta D'_{xo}\ C\alpha - \Delta D'_{yo}\ S\alpha$$

$$= C\alpha\ \{-(\theta_{zo}\ S\alpha - C\alpha)\ \Omega SL + \theta_{yo}\ \Omega CL\}\ \epsilon_L$$

$$- S\alpha\ \{-(\theta_{zo}\ C\alpha + S\alpha)\ \Omega SL - \theta_{xo}\ \Omega CL\}\ \epsilon_L$$

$$= (\Omega SL + \theta_{EO}\ \Omega CL)\ \epsilon_L \quad . \tag{74}$$

Similarly, Equations (54), (28a), and (28b) give

$$\Delta D'_{EO} = \Delta D'_{xo}\ S\alpha + \Delta D'_{yo}\ C\alpha$$

$$= S\alpha\ \{-(\theta_{zo}\ S\alpha - C\alpha)\ \Omega SL + \theta_{yo}\ \Omega CL\}\ \epsilon_L \tag{75}$$

$$+ C\alpha\ \{-(\theta_{zo}\ C\alpha + S\alpha)\ \Omega SL - \theta_{xo}\ \Omega CL\}\ \epsilon_L$$

$$= (-\theta_{zo}\ \Omega S \quad \theta_{NO}\ \Omega CL)\ \epsilon_L \quad . \tag{76}$$

It is noted that

$$\Delta\theta_{NO} = 0 \tag{77}$$

with respect to ϵ_L as can been seen from Equation (51). Substituting Equations (75), (76), and (77) into Equation (73), and neglecting all second-order terms give the error of azimuth heading in a neat equation

$$\Delta\theta_{AO} = -\epsilon_L \tan L \quad . \tag{78}$$

H. The Resultant Gyrocompassing Error

The effects of all heading-sensitive errors in gyrocompassing may now be combined. Referring to Figure 3, let the azimuth offset in the first platform position be $\alpha - 90°$ and in the second position be α. Since $\cos(\alpha - 90°) = \sin\alpha$ and $\sin(\alpha - 90°) = -\cos\alpha$, Equations (6), (58), and (71) give

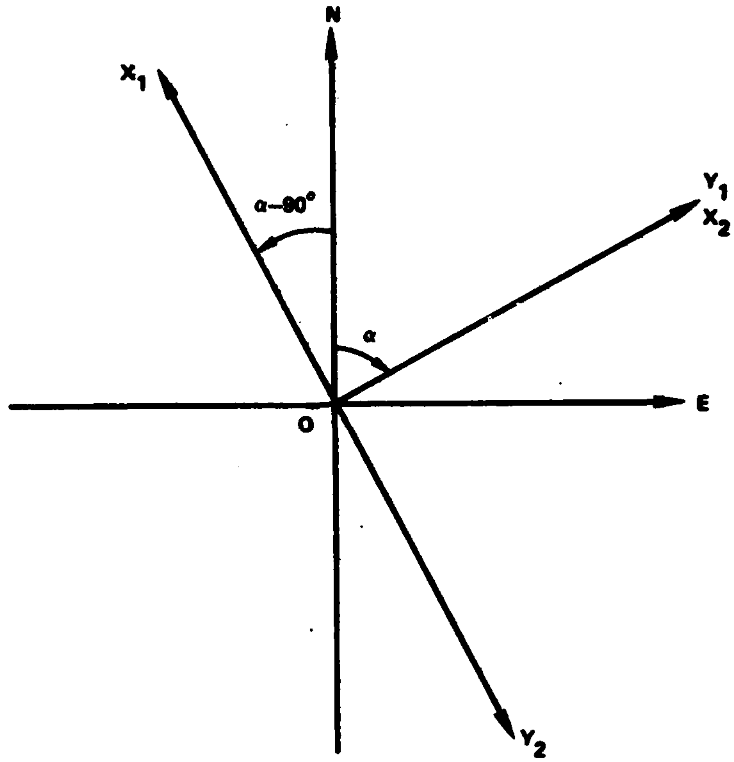

Figure 3. Two platform positions.

$$(\Delta D_N)_1 = (\Delta D'_{NO})_1 - \Delta\psi\ S\psi - (\Delta\theta_{EO})_1\ \Omega_A \approx (\Delta D'_{NO})_1 - (\Delta\theta_{EO})_1\ \Omega_A$$

$$= -\delta_{xy}\ \Omega_N\ S\alpha\ C\alpha - K_x\ \Omega_N\ C^2\alpha - K_y\ \Omega_N\ S^2\alpha$$

$$- \varepsilon_g\ \Omega_N + g\ (D_{sx}\ S\alpha + D_{sy}\ C\alpha) - (B_x\ S\alpha + B_y\ C\alpha)\ \Omega_A \qquad (79)$$

and Equation (72) gives

$$(\Delta D'_{EO})_2 = \delta_{xy}\ \Omega_N\ S^2\alpha + (K_x - K_y)\ \Omega_N\ S\alpha\ C\alpha + H_{sx}\ S\alpha + H_{sy}\ C\alpha$$

$$+ 1/2\ D_{Ixy}\ (S\alpha + C\alpha)\ g\ \Omega_N\ T + g\ (D_{sx}\ S\alpha + D_{sy}\ C\alpha) \quad . \qquad (80)$$

In Section III, it was pointed out that accelerometer bias uncertainties might be different between the first and second gyrocompassing positions. Therefore, if Equation (57) gives $\Delta\theta_{NO}$ for the first position, then for the second position

$$(\Delta\theta_{NO})_2 = -(B_x + \Delta B_x)\ S\alpha + (B_y + \Delta B_y)\ C\alpha \quad . \qquad (81)$$

The resultant gyrocompassing error is the sum of the error due to ε_L and errors due to all other sources. From Equations (7) and (78), this is given by

$$\Delta\theta_{AO} = \frac{(\Delta D^{L}_{EO})_2 - (\Delta D_N)_1}{\Omega_N} + [\varepsilon_L - (\Delta\theta_{NO})_2] \tan L \quad . \tag{82}$$

Using $(\Delta\theta_{NO})_2$ from Equation (81) and $\Delta(D_N)_1$ and $\Delta(D^{L}_{EO})_2$ from Equations (79) and (80) and noting that $\tan L = -\Omega_A/\Omega_N$ yield

$$\begin{aligned}\Delta\theta_{AO} = {} & K_x \,(S\alpha\, C\alpha + C^2\alpha) + K_y \,(S^2\alpha - S\alpha\, C\alpha) + \Delta B_x \, S\alpha \tan L \\ & + \Delta B_y \, C\alpha \tan L + H_{sx} \, S\alpha/\Omega_N + H_{sy} \, C\alpha/\Omega_N + \delta_{xy} \,(S^2\alpha + S\alpha\, C\alpha) \\ & + 1/2 \, D_{Ixy} \,(S\alpha + C\alpha)\, g \, T + \varepsilon_g + \varepsilon_L \tan L \quad .\end{aligned} \tag{83}$$

This Equation does not contain B_x, B_y, D_{sx}, and D_{sy} terms, indicating that in a first-order analysis, the azimuth heading obtained by two-position gyrocompassing is independent of fixed accelerometer bias uncertainties and spin-axis g-sensitive drifts.

Equation (83) is the final result sought. Although the object was to analyze all heading-sensitive errors, the result shows that errors due to ε_g and ε_L are not heading-sensitive as indicated in Equation (83). The set of units for various quantities in Equation (83) can be traced out through the derivation. The units are as follows:

$\Delta\theta_{AO}$ in radians

K_x and K_y in g's/g

ΔB_x and ΔB_y in g's

H_{sx} and H_{sy} in degrees per hour

δ_{xy} in radians

D_{Ixy} in (degrees per hour) per (meters per second^2)

ε_g in number of g's

ε_L in radians

Ω_N in degrees per hour

T in hours

g in meters per second^2.

A set of convenient units which is more often used in practice is given as follows:

$\Delta\theta_{AO}$ in arc minutes (arc min)

K_x and K_y in micro-g's per g (μg/g) or parts per million (ppm)

ΔB_x and ΔB_y in micro-g's (μg)

H_{sx} and H_{sy} in degrees per hour (deg/hr)

δ_{xy} in arc seconds (arc sec)

D_{Ixy} in degrees per hour per nominal g

ε_g in micro-g's (μg)

ε_L in arc seconds (arc sec)

Ω_N in degrees per hour (deg/hr)

T in seconds.

The g factor in the D_{Ixy} term is replaced by k_g with a unit in number of nominal g's where the nominal g is 9.8 m/sec^2.

Using the new set of units, Equation (83) becomes

$$\begin{aligned}\Delta\theta_{AO} = {} & k_1 \, [K_x \, (S\alpha \, C\alpha + C\alpha^2) + K_y \, (S\alpha^2 - S\alpha \, C\alpha)] \\ & + k_1 \, [\Delta B_x \, S\alpha + \Delta B_y \, C\alpha] \tan L + k_2 \, [H_{sx} \, S\alpha + H_{sy} \, C\alpha] \, /\Omega_N \\ & + k_3 \, \delta_{xy} \, [S\alpha \, C\alpha + S\alpha^2] + k_4 \, D_{Ixy} \, [S\alpha + C\alpha] \, k_g \, T + k_1 \, \varepsilon_g \\ & + k_3 \, \varepsilon_L \tan L \quad .\end{aligned} \tag{84}$$

Values of k_i, i = 1 to 4, are obtained as follows:

$$k_1 = \frac{57.3 \text{ (deg/rad)} \times 60 \text{ (arc min/deg)}}{10^6 \text{ (parts)}} = 3.438 \times 10^{-3}$$

$$k_2 = 57.3 \text{ (deg/rad)} \times 60 \text{ (arc min/deg)} = 3438$$

$$k_3 = \frac{57.3\ (\text{deg/rad}) \times 60\ (\text{arc min/rad})}{57.3\ (\text{deg/rad}) \times 3600\ (\text{sec/deg})} = 1/60$$

$$k_4 = 1/2 \times \frac{57.3\ (\text{deg/rad}) \times 60\ (\text{arc min/deg}) \times 9.8\ (\text{m/sec}^2)}{60\ (\text{min/deg}) \times 3600\ (\text{sec/hr})} = 0.07799$$

k_g is 9.8 m/sec^2.

I. A Sample Calculation

To illustrate the nature of the heading sensitivity of individual error components and their contribution to the resultant heading error, a sample case in computed using the following set of parameter values.

$K_x = K_y = 100$ ppm

$\Delta B_x = \Delta B_y = 100\ \mu g$

$H_{sx} = H_{sy} = 0.001$ deg/hr

$\delta_{xy} = 10$ arc sec

$D_{Ixy} = 0.0015$ deg/hr/g

$\varepsilon_g = -10\ \mu g$

$\varepsilon_L = -10$ arc sec

$k_g = 0.999665$

$\Omega = 15$ deg/hr

$L = 34.6425°$

$T = 240$ sec .

Figure 4 shows the variation of individual heading errors as a function of nominal heading angle α. Figure 5 shows the variation of the resultant heading error. All individual errors have sinusoidal variations except those due to ε_g and ε_L. Errors due to ε_g and ε_L have constant values indicating their insensitivity to heading. Errors due to K_x, K_y, and δ_{xy} have non-zero means, while those due to ΔB_x, ΔB_y, H_{sx}, H_{sy}, and D_{Ixy} have zero means.

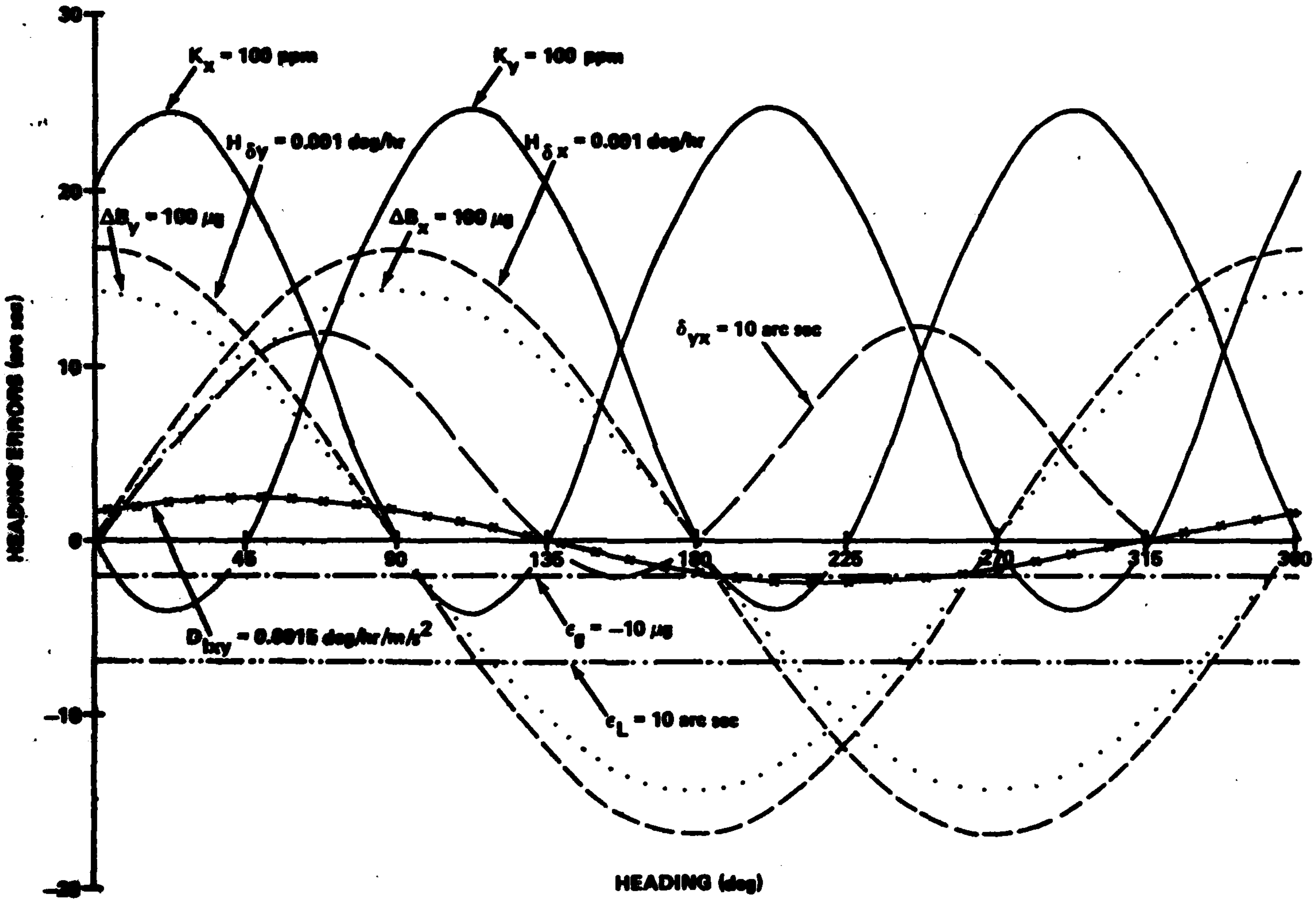

Figure 4. Individual heading errors.

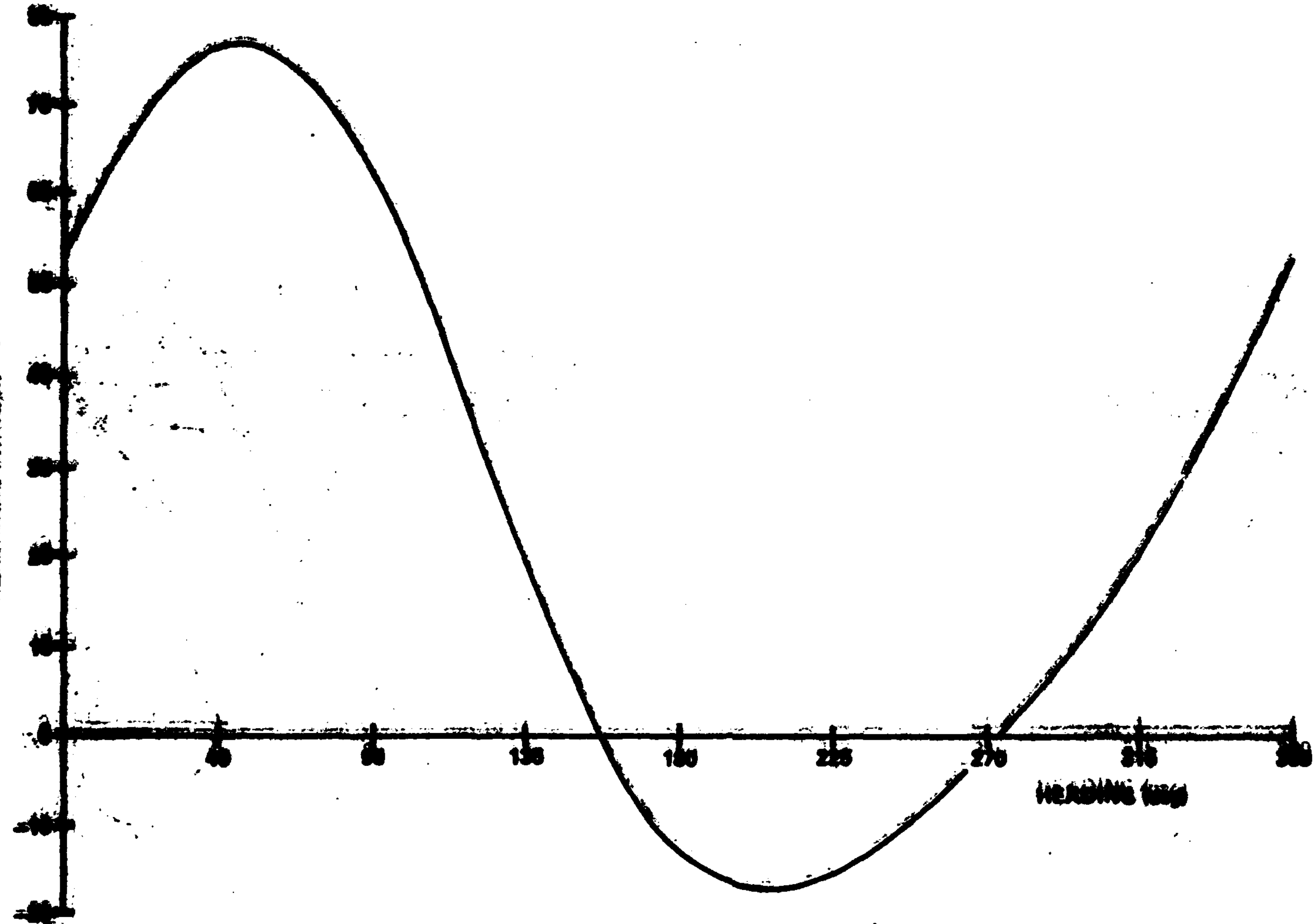

Figure 5. Resultant heading error.

By examining Figure 5 it is seen that gyrocompassing error is smaller for certain headings than for others. This phenomenon suggests that, for each IMU, a nominal heading position α can be identified which gives the best gyrocompassing accuracy.

V. ERROR DUE TO BASE MOTION

Base motion is a random process which is low frequency in nature as compared to the instrument noise; therefore, it is colored. Its effect on the accuracy of gyrocompassing depends on the details of the data processing algorithm used. Experiments with two different algorithms are presently under way. The first one involves the use of a conventional least-square polynomial fit formula to fit two second-order polynomials [12]. The second algorithm employs a parameter-correlated least-square regression to fit a set of two third-order polynomials [2,3,5,6,7]. Here the error analysis is performed based on the first algorithm.

Equations (3) and (4) are seen to be third-order polynomials in t. The first algorithm uses the following approximation at the outset

$$V = a + bt + ct^2 \quad . \tag{85}$$

The determination of heading is dominated by the first term of gyrocompassing Equation (7). Therefore, the accuracy of gyrocompassing primarily relies on the determination of drift which is proportional to the coefficient c of the t^2-term in Equation (85). The present analysis will be concentrated on the c coefficient.

The conventional least-square regression for a second-order polynomial is to minimize

$$I = \int_0^t \left[V(t) - (a + bt + ct^2)\right]^2 dt \quad . \tag{86}$$

Letting $\frac{\partial I}{\partial a} = \frac{\partial I}{\partial b} = \frac{\partial I}{\partial c} = 0$ and performing several integrations of the polynomial give

$$\begin{bmatrix} I_1 \\ I_2 \\ I_3 \end{bmatrix} = \begin{bmatrix} T & \frac{T^2}{2} & \frac{T^3}{3} \\ \frac{T^2}{2} & \frac{T^3}{3} & \frac{T^4}{4} \\ \frac{T^3}{3} & \frac{T^4}{4} & \frac{T^5}{5} \end{bmatrix} \begin{bmatrix} a \\ b \\ c \end{bmatrix} \tag{87}$$

where

$$I_1 = \int_0^t V dt \tag{88a}$$

$$I_2 = \int_0^t V t dt \tag{88b}$$

$$I_3 = \int_0^t V t^2 dt \quad . \tag{88c}$$

Solving Equation (84) for the coefficient C gives

$$C = \frac{30}{T^3} I_1 - \frac{180}{T^4} I_2 + \frac{180}{T^5} I_3 \quad . \tag{89}$$

Squaring Equation (89) gives

$$C^2 = \left(\frac{30}{T^3}\right)^2 I_1{}^2 + \left(\frac{180}{T^4}\right)^2 I_2{}^2 + \left(\frac{180}{T^5}\right)^2 I_3{}^2$$
$$- \frac{10800}{T^7} I_1 I_2 + \frac{10800}{T^8} I_1 I_2 - \frac{64800}{T^9} I_2 I_3 \tag{90}$$

which will be used later for obtaining the standard deviation of C. The base motion error will be analyzed by first using a velocity model and then an acceleration model.

A. Analysis via Velocity Model

It is assumed that the velocity of base motion has the following model:

$$V = \sum_{n=1}^{N} A_n \sin (\omega_n t + \phi_n) \quad . \tag{91}$$

This amounts to representing the velocity by its Fourier components. Using Equation (91) in Equation (88) yields

$$I_1 = \sum_{n=1}^{N} \left(\frac{A_n}{\omega_n}\right) \left\{ \cos \phi_n - \cos (\omega_n t + \phi_n) \right\} \tag{92a}$$

$$I_2 = \sum_{n=1}^{N} \left(\frac{A_n}{\omega_n^2}\right) \left\{ \sin (\omega_n t + \phi_n) - \sin \phi_n - \omega_n t \cos (\omega_n t + \phi_n) \right\} \tag{92b}$$

$$I_3 = \sum_{n=1}^{N} \left(\frac{A_n}{\omega_n^3}\right) \Big\{ 2 \cos \phi_n - 2 \cos (\omega_n t + \phi_n)$$

$$+ 2 \omega_n t \sin (\omega_n t + \phi_n) - \omega_n^2 t^2 \cos (\omega_n t + \phi_n) \Big\} \quad . \tag{92c}$$

Squaring Equation (92a) and dropping cross-frequency product terms yield

$$I_1^2 = \left\{ \sum_{n=1}^{N} \left(\frac{A_n}{\omega_n}\right) \left[\cos \phi_n - \cos (\omega_n t + \phi_n) \right] \right\}^2$$

$$= \sum_{n=1}^{N} \left(\frac{A_n}{\omega_n}\right)^2 \left\{ \cos^2 \phi_n + \cos^2 (\omega_n t + \phi_n) - 2 \cos \phi_n \cos (\omega_n t + \phi_n) \right\}$$

$$= \sum_{n=1}^{N} \left(\frac{A_n}{\omega_n}\right)^2 \Big\{ \frac{1 + \cos 2 \phi_n}{2} + \frac{1 + \cos 2 (\omega_n t + \phi_n)}{2}$$

$$+ 2 \cos \phi_n \cos (\omega_n t + \phi_n) \Big\} \quad . \tag{93}$$

The cross-frequency product terms are dropped because their average values are zero. Again, all terms in Equation (93) which have a zero time-average are discarded:

$$I_1^2 = \sum_{n=1}^{N} \left(\frac{A_n}{\omega_n}\right)^2 \left(\frac{1}{2} + \frac{1}{2} + \frac{\cos^2 \phi_n}{2}\right) \leq \frac{3}{2} \sum_{n=1}^{N} \left(\frac{A_n}{\omega_n}\right)^2 \tag{94a}$$

To be conservative, let

$$I_1^2 = \frac{3}{2} \sum_{n=1}^{N} \left(\frac{A_n}{\omega_n}\right)^2 \quad . \tag{94b}$$

Similar considerations produce

$$I_2^2 = \frac{T^2}{2} \sum_{n=1}^{N} \left(\frac{A_n}{\omega_n}\right)^2 \tag{94c}$$

$$I_3^2 = \frac{T^4}{2} \sum_{n=1}^{N} \left(\frac{A_n}{\omega_n}\right)^2 \quad . \tag{94d}$$

$$I_1\, I_2 = \frac{T}{2} \sum_{n=1}^{N} \left(\frac{A_n}{\omega_n}\right)^2 \tag{94e}$$

$$I_2\, I_3 = \frac{T^3}{2} \sum_{n=1}^{N} \left(\frac{A_n}{\omega_n}\right)^2 \tag{94f}$$

$$I_3\, I_1 = \frac{T^2}{2} \sum_{n=1}^{N} \left(\frac{A_n}{\omega_n}\right)^2 \quad . \tag{94g}$$

When Equation (94) is substituted into Equation (91), several terms cancel each other. The result is the time-average of C^2:

$$\overline{C^2} = \frac{3}{2}\left(\frac{30}{T^3}\right)^2 \sum_{n=1}^{N} \left(\frac{A_n}{\omega_n}\right)^2 \quad . \tag{95}$$

Assuming ergodicity, time-average equals ensemble average and Equation (95) gives $\sigma_C{}^2$, the variance of C. Since the north and east channels of the platform are similar, the following is obtained:

$$\sigma_{C_N}{}^2 = \sigma_{C_E}{}^2 = \frac{3}{2}\left(\frac{30}{T^3}\right)^2 \sum_{n=1}^{N} \left(\frac{A_n}{\omega_n}\right)^2 \quad . \tag{96}$$

Coefficients C_N and C_E are related to drifts by

$$D'_{NO} = -2\, C_E \tag{97a}$$

and

$$D'_{EO} = 2\, C_N \tag{97b}$$

which can be obtained by comparing Equation (85) to Equations (3) and (4). The standard deviation of the heading error can be obtained from Equations (7) and (97) as

$$\sigma_{\theta_A} = \frac{2\sqrt{\sigma_{C_N}{}^2 + \sigma_{C_E}{}^2}}{\Omega \cos L} \tag{98}$$

where the second term of Equation (7) has been neglected. Using Equation (96) in Equation (98)

$$\sigma_{\theta_A} = \sqrt{3}\left(\frac{30}{T^3}\right)\sqrt{\sum_{n=1}^{N}\left(\frac{A_n}{\omega_n}\right)^2}\,\frac{2}{\Omega \cos L}\ \text{rad} \tag{99}$$

or

$$\sigma_{\theta_A} = \frac{2\sqrt{3}}{\Omega \cos L}\left(\frac{30}{T^3}\right)\sqrt{\sum_{n=1}^{N}\left(\frac{A_n}{\omega_n}\right)^2}\ (57.3 \times 60)\ \text{arc min} \tag{100}$$

Equation (100) shows that the error due to base motion decreases with frequency ω_n and time T over which least-squares regression is done. Also, the base motion error is larger at higher latitude.

B. Analysis via Acceleration Model

The acceleration model for the base motion is assumed to be

$$a = \sum_{n=1}^{N} G_n\ (\omega_n t + \phi_n) \quad . \tag{101}$$

Following a similar derivation as that for the velocity model yields

$$I_1^{\,2} = \frac{3}{2}\sum_{n=1}^{N}\left(\frac{G_n}{\omega_n^2}\right)^2 \tag{102a}$$

$$I_2^{\,2} = \frac{T^2}{2}\sum_{n=1}^{N}\left(\frac{G_n}{\omega_n^2}\right)^2 \tag{102b}$$

$$I_3^{\,2} = \frac{T^4}{2}\sum_{n=1}^{N}\left(\frac{G_n}{\omega_n^2}\right)^2 \tag{102c}$$

$$I_1\ I_2 = \frac{T}{2}\sum_{n=1}^{N}\left(\frac{G_n}{\omega_n^2}\right)^2 \quad . \tag{102d}$$

$$I_2 I_3 = \frac{T^3}{2} \sum_{n=1}^{N} \left(\frac{G_n}{\omega_n^2}\right)^2 \tag{102e}$$

$$I_3 I_1 = \frac{T^2}{2} \sum_{n=1}^{N} \left(\frac{G_n}{\omega_n^2}\right)^2 \quad . \tag{102f}$$

Substituting Equation (98) into Equation (87) and simplifying the result give the time-average of C^2:

$$\overline{C^2} = \frac{3}{2}\left(\frac{30}{T^3}\right)^2 \sum_{n=1}^{N} \left(\frac{A_n}{\omega_n^2}\right)^2 \quad . \tag{103}$$

Using the same reasoning as used in getting Equation (100) the heading error standard deviation is given as

$$\sigma_{\theta_A} = \frac{2\sqrt{3}}{\Omega \cos L}\left(\frac{30}{T^3}\right) \sqrt{\sum_{n=1}^{N} \left(\frac{G_n}{\omega_n^2}\right)^2} \; (57.3 \times 60) \text{ arc min} \quad . \tag{104}$$

C. A Sample Computation

Consider

$$\omega_o = n\, \omega_o \tag{105}$$

where $\omega_o = \pi$ rad/sec and n = 1 to 100. Let

$G_n = 2 \times 10^{-3}$ g for all n

T = 240 sec

L = 34.6425°

$\Omega = 7.29211 \times 10^{-5}$ rad/sec .

Equation (100) gives the heading error standard deviation

$\sigma_{\theta_A} = 5.45$ arc sec .

VI. CONCLUSION

There are three categories of gyrocompassing errors. Analysis for the first two categories has been treated in this report; the third category has been reported elsewhere by the authors. The analysis has been beneficial in three ways. It offered an opportunity for a better understanding of the underlying principle governing each error source. The analytic expressions obtained enable an estimation of gyrocompassing error with known error sources. It also provided a model which can be used to develop identification techniques for error sources based on test data.

Errors of the first category include all those which are short-term stationary. A deterministic type of analytic expression, Equations (83) or (84), for heading error was obtained for this category. Using this expression, identification of error sources can be devised. By compensating for the identified error sources, gyrocompassing accuracy can be improved. A scheme for accomplishing this will appear in a later paper.

Errors of the second category result from base motions which are random and time-varying disturbances. Their effect on gyrocompassing accuracy has been analyzed statistically. Analytic expressions in Equations (100) and (104) give the standard deviation of heading error in terms of spectral properties of the base motion. Error sources of this type cannot be compensated by adjusting hardware parameters. However, their effect can be minimized by using a proper data processing algorithm. The low-frequency nature of these types of disturbances implies that they are not white; therefore, they are more difficult to filter than white noise.

The third category of error sources includes all instrument noise which usually can be approximated as white noise. A statistical analysis for this category has been reported elsewhere recently and is not detailed in this report. The effect of this type of noise on gyrocompassing accuracy can be reduced by proper filtering.

Finally, it should be pointed out that a fourth category of error sources has not been mentioned in this report. This category includes all software errors such as round-off error, truncation error, and errors induced by approximations made during algorithm development. This last category of errors will be treated in the future.

REFERENCES

1. Hung, J. C. and White, H. V., IMU Self-Alignment Techniques, US Army Missile Command, Redstone Arsenal, Alabama, September 1974, Report No. RG-75-15.

2. Hung, J. C. and White, H. V., "Parameter Correlated Least Square Regression Algorithm," Proceedings of Asilomar Conference Circuits, Systems and Computers, Pacific Grove, California, 3-5 December 1974, pp. 415-419.

3. Hung, J. C. and White, H. V., "Error Analysis for Parameter Correlated Least Square Regression Algorithm," Proceedings of 1975 Southeastern Symposium on System Theory, Auburn and Tuskegee, Alabama, 20-21 March 1975.

4. White, H. V., Description of Two-Axis Table Method for Pershing II Inertial Measurement Unit Gyrocompassing Verification, US Army Missile Command, Redstone Arsenal, Alabama, June 1975, Report No. RG-75-57.

5. Hung, J. C. and White, H. V., "On IMU Self-Alignment Algorithms," Proceedings of the Sixth Triennial World Congress of the International Federation of Automatic Control, Instrument Society of America, Pittsburg, Pennsylvania, August 1975.

6. Hung, J. C. and White, H. V., More On IMU Self-Alignment Techniques, US Army Missile Command, Redstone Arsenal, Alabama, September 1975, Report No. RG-76-23.

7. Hung, J. C. and White, H. V., "Self-Alignment Techniques for Inertial Measurement Units," IEEE Transactions on Aerospace and Electronic Systems, Vol. AES-11, No. 6, November 1975.

8. Hung, J. C. and White, H. V., "An Efficient Inertial Measurement Unit (IMU) Alignment Software," Proceedings of the IEEE Position Location and Navigation Symposium (PLANS 76), IEEE Publication 76CH1138-7 AES, New York, New York, 1-3 November 1976, pp. 128-132.

9. White, H. V., Pershing PII Inertial Measurement Unit Field Gyrocompassing Test, US Army Missile Research and Development Command, Redstone Arsenal, Alabama, June 1977, Report No. TG-77-16.

10. White, H. V. and Hung, J. C., "Field Test and Data Analysis for PII IMU Gyrocompassing," Proceedings of the IEEE Position Location and Navigation Symposium (PLANS 78), San Diego, California, 7-9 November 1978.

11. White, H. V. and Hung, J. C., "Analysis of Heading-Sensitive Gyrocompassing Errors," Proceedings of 25th International Instrumentation Symposium, Anaheim, California, 7-10 May 1979.

12. Danik, B., Gyrocompassing Alignment of Inertial Platform, The Singer Co., Kearfott Division, 6 February 1973, Document No. KD-73-9.

DISTRIBUTION

	No. of Copies
Defense Documentation Center Cameron Station Alexandria, Virginia 23144	12
Commander US Army Materiel Development and Readiness Command	
Attn: DRCRD	1
DRCDL	1
5001 Eisenhower Avenue Alexandria, Virginia 22333	
The University of Tennessee Department of Electrical Engineering	
Attn: Dr. J. C. Hung	1
Knoxville, Tennessee 37916	
NASA Johnson Space Center EG5	
Attn: Mr. Malcolm Jones	1
Houston, Texas 77058	
Southern Technologies, Inc.	
Attn: T. Ward	1
110 Wynn Drive Huntsville, Alabama 35805	
DRCPM-PE-E, Mr. Pettitt	1
-PE-EA, Mr. Wagner	1
Mr. Gregory	1
DRSMI-LP, Mr. Voigt	1
DRDMI-X, Mr. McKinley	1
-T, Dr. Kobler	1
-TG	1
-TGL, Mr. White	5
-TGG, Mr. Ciliax	1
-TGN, Mr. McLean	1
-ESL, Mr. Graham	1
-TBD	3
-TI (Record Set)	1
(Reference Copy)	1